

In silico exploration of bioactive secondary metabolites with anesthetic effects on sodium channels Nav 1.7, 1.8, and 1.9 in painful human dental pulp

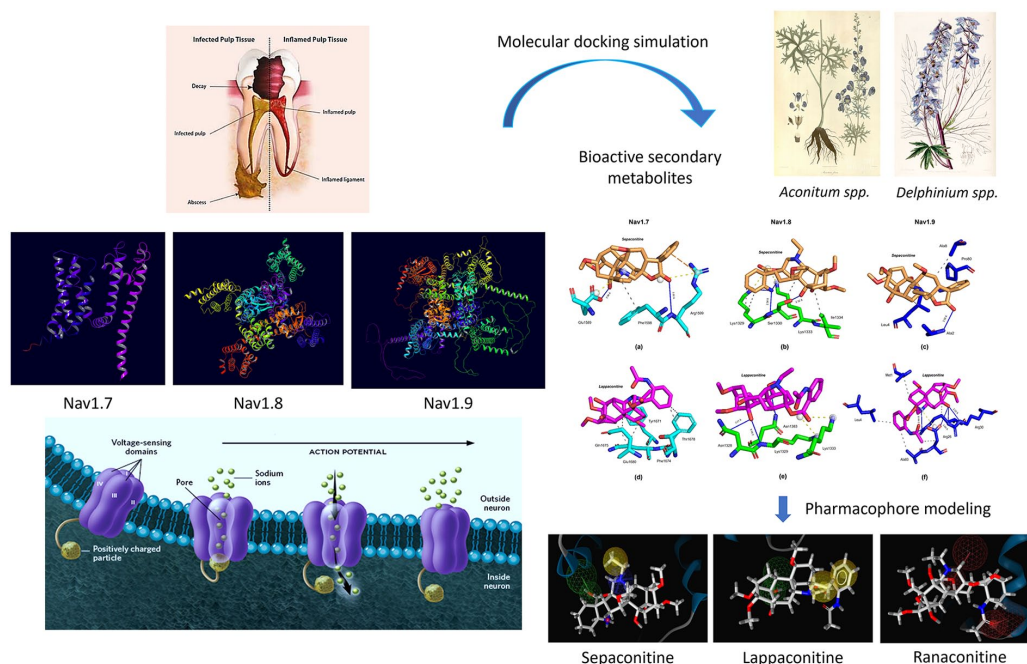
Molecular Pain
Volume 21: 1–22
© The Author(s) 2025
Article reuse guidelines:
sagepub.com/journals-permissions
DOI: 10.1177/17448069251327824
journals.sagepub.com/home/mtx
S Sage

Ravinder S Saini¹, Rayan Ibrahim H Binduhayyim¹,
Mohamed Saheer Kuruniyan¹, and Artak Heboyan² 

Abstract

Aim: To investigate the efficacy of medicinal plant bioactive secondary metabolites as inhibitors of voltage-gated sodium channels (Nav1.7, Nav1.8, and Nav1.9) in managing painful states of dental pulps. **Methodology:** Molecular docking, ADME prediction, toxicity profiling, and pharmacophore modeling were used to assess the binding affinities, pharmacokinetic properties, toxicological profiles, and active pharmacophores of the selected bioactive compounds. **Results:** Three compounds (Sespaconitine, Lappaconitine, and Ranaconitine) showed binding affinities ($\Delta G = -8.95$ kcal/mol, -7.77 kcal/mol, and -7.44 kcal/mol, respectively) with all three Nav1.7, Nav1.8, and Nav1.9 sodium channels. The sespaconitine amine group formed hydrophobic interactions with key residues. The Lappaconitine benzene ring contributed to hydrophobic interactions and hydrogen bond acceptor interactions. The hydrophobic interactions of the ranaconitine amine group play a critical role with specific residues on Nav1.8 and Nav1.9. **Conclusion:** The natural fusicoccane diterpenoid derivatives Sespaconitine, Lappaconitine, and Ranaconitine are potential lead compounds for the development of novel analgesics as selective antihyperalgesic drugs, which will provide a new dental pharmacological intervention for managing painful dental pulp conditions. Further experimental validation and clinical studies that confirm the efficacy and safety of these compounds will strengthen their applicability in dental practice.

Graphical abstract



Keywords

Anesthetic, dental pulp, molecular docking, pharmacophore, voltage-gated sodium channels

Date received: 14 November 2024; revised 16 January 2025; accepted: 27 February 2025

Introduction

Dental pulp pain is a highly prevalent clinical problem, a type of acute and often severe odontogenic pain that arises from the innermost region of the tooth known as the dental pulp.¹ Such nociceptive pain typically reflects conditions, such as dental decay, trauma, or infection. This pain mechanism is called “nociception,” as it tracks destructive changes in the body. The nervous system anatomy involves the activation of pain pathways.² Voltage-gated sodium channels, particularly Nav1.7, Nav1.8, and Nav1.9, are important for the conduction of pain signals from the dental pulp to the central nervous system, because they are highly expressed in the peripheral nervous system and are implicated in the coding of pain.^{3,4} Nav1.7 is most highly expressed in peripheral neurons and is critical for setting the firing threshold for pain signals. Loss-of-function mutations in SCN9A, the gene encoding Nav1.7, cause congenital insensitivity to pain, while gain-of-function mutations cause severe pain disorders like erythromelalgia.^{5,6} This emphasizes the importance of Nav1.7 in the initiation of pain signals. Nav1.8 is another leading channel in pain pathways and has been predominantly identified in pathologies that cause inflammatory and neuropathic pain. This channel is resistant to tetrodotoxin, a strong inhibitor of the sodium channel, and therefore, remains active even under conditions that inhibit other channels. Nav1.8 seems to be involved in transmitting pain signals, particularly in the C-fibers, which are responsible for slow, chronic pain signals, seems to be involved in the transmission of pain signals. Its role is enhanced under conditions of inflammation, and it remains a major focus as a therapeutic target for inflammatory pain.^{7,8} Nav1.9 is less well characterized but has been shown to regulate the excitability (driving force) of nociceptors – sensory neurons that encode potentially damaging stimuli. Mutations in the SCN11A gene encoding Nav1.9 are associated with pain insensitivity and other pain-related disorders, and contribute to the maintenance of pain in chronic pain conditions.^{9–11} Collectively, these channels provide several new targets for the development of novel analgesic and anesthetic drugs that provide more targeted and potent pain management.

At present, clinical anesthetics, such as lidocaine and bupivacaine, are widely used to relieve pain in dental practice.

These anesthetics function primarily by blocking voltage-gated sodium channels, particularly those involved in the transmission of pain signals, such as Nav1.7, Nav1.8, and Nav1.9. These sodium channels play critical roles in the initiation and propagation of nerve impulses by regulating the flow of sodium ions into the nerve cells, which is essential for the generation and conduction of action potentials. By inhibiting these channels, lidocaine and bupivacaine prevent the initiation and propagation of pain signals from the dental pulp to the brain, leading to localized numbness in the target area.^{12,13} However, this lack of specificity may lead to adverse effects. By failing to selectively target pain-specific sodium channels, they affect neurons broadly, which leads to a constellation of side effects, including neuropathic symptoms such as non-site-specific numbness, motor complications, and systemic toxicity at higher doses.^{14,15} Moreover, these anesthetics have a relatively short duration of action.¹⁶ Lidocaine, for example, typically has an onset of action of about 1–2 h, and bupivacaine, a longer-lasting anesthetic, has an onset of action of as long as several hours, but carries a higher risk of cardiotoxicity. Because of this short duration, repeated administration is frequently required throughout long dental procedures that add to patient discomfort and risk of adverse effects.¹⁷ Additionally, the risk of allergic reactions and/or loss of efficacy owing to tolerance or sensitization with repeated use makes their use problematic.¹⁸ These limitations highlight the need for novel anesthetic agents that can deliver prolonged, effective pain relief while minimizing unwanted side effects, particularly through the selective targeting of pain-related sodium channels.

In response to these challenges, bioactive secondary metabolites from natural sources, such as plants, fungi, and microorganisms, present a promising alternative. These compounds, including alkaloids, terpenoids, and flavonoids, offer potent pharmacological activities, including the modulation of ion channels like sodium channels, which are crucial in pain management. Bioactive secondary metabolites are produced by plants, fungi, or microorganisms, but are not involved in primary metabolic processes. They encompass a wide variety of compounds such as alkaloids, terpenoids, and flavonoids, and have been found to possess considerable pharmacological activities. They are a great source of new anesthetic drugs.^{19,20} Alkaloids such as morphine and quinine

¹Department of Allied Dental Health Sciences, COAMS, King Khalid University, Abha, Saudi Arabia

²Department of Prosthodontics, Faculty of Stomatology, Yerevan State Medical University after Mkhitar Heratsi, Yerevan, Armenia

Corresponding Author:

Artak Heboyan, Department of Prosthodontics, Faculty of Stomatology, Yerevan State Medical University after Mkhitar Heratsi, Str. Koryun 2, Yerevan 0025, Armenia.

Email: heboyan.artak@gmail.com

have long been used for their analgesic properties. Their ability to modulate ion channels, including sodium channels, makes them potential candidates for anesthetic agent development.^{21,22} Terpenoids are the major components of essential oils and other plant extracts, and have robust anti-inflammatory and pain-relieving effects. Menthol and camphor have been used topically for these purposes in traditional medicine.^{23,24} Flavonoids, a major class of plant-based antioxidants and anti-inflammatory compounds present in fruits and vegetables, inhibit certain subtypes of sodium channels, thereby rendering neurons less excitable and less responsive to pain stimuli. For example, quercetin, a flavonoid found in apples, onions, and berries, selectively inhibits pain-sensitive sodium channels.²⁵ Rutin, a flavonoid found in citrus fruits and buckwheat, exhibits similar properties, making it a candidate for further exploration as a natural pain-relieving agent.²⁶ The diverse chemical structures and mechanisms of action of these metabolites provide rich resources for the discovery of novel compounds that can target specific sodium channels with high efficacy and safety.

Using *in silico* approaches, insightful tools are now in place to predict and characterize the interactions between new drug candidates and their targets.^{27,28} A key approach is molecular docking, which models the accommodated binding of small molecules to a selected target protein, such as a sodium channel, for each compound's best fit and affinity.^{29,30} This indicates that the candidates are likely to maximize efficacy. The second approach to complement docking is pharmacophore modeling, which identifies the appropriate spatial arrangement of features essential for optimal target binding, thereby guiding the design of new molecules with these properties.^{31,32} Secondly, *in silico* approaches include the prediction of Absorption, Distribution, Metabolism, and Excretion (ADME) properties, which determine the pharmacokinetic characteristics of a compound to ensure that it reaches its target safely inside the body.³³ Drug-likeness screening then assesses whether a compound has the characteristics that would need to be made into a drug, including stability, solubility, and permeability.³⁴ Toxicity prediction models reflect adverse effects as early as the discovery phase of drug development, helping prevent failed late-stage trials.³⁵ Therefore, the major objective of the current study was to evaluate the potential of bioactive secondary metabolites as promising novel anesthetic compounds acting on the voltage-gated sodium channel subtypes Nav1.7, Nav1.8, and Nav1.9 via molecular docking.

By evaluating the compounds that bind most strongly and with the right interactions to these channels, this study could lead to the design of dental anesthetics. The team is hoping that computational methods will speed up discovery and help reveal more about the mechanisms of action of natural compounds.

Methodology

Data selection and ligand structure development of bioactive secondary metabolites

This study was performed using proper resolution structural data for the human voltage-gated sodium channels Nav1.7, Nav1.8, from the Protein Data Bank (PDB): Nav1.7 (crystal structure, X-ray resolution): PDB ID: 5EK0³⁶) resolution: 3.53 Å; Nav1.8 (crystal structure, X-ray resolution): PDB ID: 7WE4³⁷) resolution: 2.70 Å. Because no experimentally determined structure of Nav1.9 has been deposited in the PDB, a model of Nav1.9 was generated from AlphaFold.³⁸ Before any simulations, the PDB files of each sodium channel were first refined in Swiss-PDB Viewer 4.1³⁹ to fill in any missing residues. This is necessary to maintain the structural integrity of protein models. The prepared protein structures were then uploaded to the BioVIA Discovery Studio Visualizer 2021 and prepared for docking simulations. Water molecules, heteroatoms, and co-crystallized ligands were removed as they may interfere with the docking simulations. Polar hydrogens were added, and Kollman charges were assigned to the proteins to capture the electrostatic properties of the biologically active sites. The CASTp 3.0 technique was adopted to identify the active sites of these receptors. CASTp (Computed Atlas of Surface Topography of Proteins) detects the size and shape of protein surface cavities and pockets. It measures the size of each detected cavity, identifies the location of the cavities, and provides precise coordinates of the cavities. CASTp is a powerful and reliable computational tool for macromolecular analysis and plays an important role in chemical and biological studies.⁴⁰ This tool was fundamental to pinpointing the active sites of Nav1.7, Nav1.8, and modeled Nav1.9, which is critical for effective docking simulations.

The sophisticated crystal structures of these secondary metabolites are crucial templates for understanding the molecular interplay between human sodium channels and their cognate bioactive ligands. The selection of bioactive secondary metabolites was based on a comprehensive literature survey focusing on compounds that could inhibit sodium channels. The primary sources for scientific investigation were peer-reviewed journals and digital data warehouses accessible through databases such as PubMed, Scopus, the World Health Organization (WHO) website, and Google Scholar, which were excluded to maintain a high standard of data reliability. Only scientifically rigorous publications, including peer-reviewed journals and WHO-edited case reports, were considered, resulting in a curated list of secondary metabolites (Table 1). Their molecular structures were obtained from PubChem (<https://pubchem.ncbi.nlm.nih.gov/>) and maintained in the National Library of Medicine. To ensure the accuracy of these structures, they were further refined and optimized using Chem3D software (PerkinElmer,

Table 1. Anesthetic activities and bioactive secondary metabolites of various medicinal plants.

Plant name	Bioactive secondary metabolite	Anesthetic activity/dose	Ref
Essential oils and terpenoids			
Peppermint (<i>Mentha piperita</i>)	Menthol, Camphor	Reduced electrically evoked contractions of rat phrenic nerve-hemidiaphragm at 0.1–100 ng/mL. Increased number of stimuli required to evoke rabbit conjunctival reflex at 10–100 µg/mL.	60,61
Lavender (<i>Lavandula angustifolia</i>)	Linalool	Reduced electrically evoked contractions of rat phrenic-hemidiaphragm. Depressed rabbit conjunctival reflexes. Reversely blocked the excitability of rat sciatic nerves and inhibited the voltage-gated Na ⁺ currents of rat dorsal root ganglion neurons.	62,63
Marjoram (<i>Origanum majorana</i>)	α-Terpineol	Reduced electrically evoked contractions of rat phrenic nerve-hemidiaphragm. Increased the number of stimuli required to evoke rabbit conjunctival reflex.	64
Anise (<i>Pimpinella anisum</i>)	Anethole	Reduced electrically evoked contractions of rat phrenic nerve-hemidiaphragm. Increased the number of stimuli required to evoke rabbit conjunctival reflex.	64
Myrrh (<i>Commiphora molmol</i>)	Furanodiene, Methoxyfuranoguaia-9-ene-8-one	A specified fraction with anesthetic potency by a rabbit conjunctival reflex test. Identified furanodiene-6-one and methoxyfuranoguaia-9-ene-8-one as active components.	65
Clove (<i>Syzygium aromaticum</i>)	β-Caryophyllene	Exerted local anesthetic effects comparable to procaine. Reduced electrically evoked contractions of rat phrenic nerve-hemidiaphragm. Increased number of stimuli necessary to provoke rabbit conjunctival reflex.	66
Alkaloids			
Monkshood (<i>Aconitum spp.</i>)	Aconitine, Lappaconitine, Bulleyaconitine A	Greater potency and longer duration of anesthesia than procaine and lidocaine. Intravenously administered samples to mice showed antinociceptive effects.	67–69
Larkspur (<i>Delphinium spp.</i>)	Sepaconitine, Ranaconitine, Sarcorine	Greater potency and longer duration of anesthesia than procaine and lidocaine.	68
Cinchona tree (<i>Cinchona spp.</i>)	Quinine	Inhibition of the K ⁺ /H ⁺ exchanger in respiring mitochondria, while not affecting the Na ⁺ /H ⁺ exchanger, inhibits K ⁺ efflux via the K ⁺ /H ⁺ exchanger.	70
Thyme (<i>Thymus vulgaris</i>)	Tetrahydroharman, Tetrahydronorharman, Thymol, Eugenol	Interacted with biomimetic membranes to increase membrane fluidity at high micromolar concentrations. Counteracted mechanistic membrane effects of local anesthetics.	22
Flavonoids and stilbenoids			
Red Wine (<i>Vitis spp.</i>)	Quercetin, Catechin, Rutin, Epicatechin, Anthocyanins	It inhibits voltage-gated Na ⁺ , K ⁺ , and Ca ²⁺ channels with IC ₅₀ values of 2.5, 4.0, and 0.8–1.5 µg/mL, respectively.	71
Green Tea (<i>Camellia sinensis</i>)	Epigallocatechin-3-gallate, Epigallocatechin	Potent inhibition of both TTX-sensitive and TTX-resistant Na ⁺ currents.	72
Bitter kola (<i>Garcinia kola</i>)	Kolaflavanone	10 mg/mL (i.d.) induced 92% local anesthesia, comparable to lidocaine (0.66 mg/kg, i.d.).	73
Japanese knotweed (<i>Fallopia japonica</i>)	Resveratrol	Both TTX-sensitive and TTX-resistant Na ⁺ currents were suppressed in rat dorsal root ganglion neurons.	74

Inc.). Energy minimization was performed using the MM2 force field in ChemDraw Professional 20.1.1 (PerkinElmer Inc.), which helps achieve a stable and low-energy conformation of the ligands, which is essential for reliable docking results.^{41,42} This meticulous preparation of protein and ligand structures sets the stage for subsequent molecular docking simulations. After docking, binding orientations and affinities were predicted for the secondary metabolites of each target sodium channel, providing a brief glimpse of their anesthetic potential. Subsequently, interaction analyses were performed to establish the detailed binding modes and

patterns leading to blocking of the sodium channels Nav1.7, Nav1.8, and Nav1.9.

Molecular docking simulation

Molecular docking was conducted using the High Ambiguity Driven Protein-Protein Docking (HADDOCK) standalone version,⁴³ leveraging the advanced interface option. This advanced software allowed protein-ligand docking to be performed at high resolution and enabled visualization of the intricate protein-ligand interactions

between the bioactive secondary metabolites and human sodium channels, which would act as receptor targets. The active site features for the sodium channels were extracted from the CASTp analysis and used as inputs to perform protein-ligand docking. For HADDOCK docking simulations, a scoring threshold of -10.00 kcal/mol was applied to select the most favorable docking poses based on binding affinity. Two main criteria guided the selection of the top protein-ligand docking results for each complex. We first selected the results with the largest number of clusters/populations (clusters of protein complexes), indicating the confidence of the docking prediction. Subsequently, we selected the results with the highest docking scores according to the HADDOCK score (a trusted value for the binding affinity between the proteins and ligands in a complex). The scoring function used by HADDOCK considers both the electrostatic and van der Waals interactions between the protein and ligand, the desolvation energies, and any changes in the conformational flexibility of the ligand and receptor.^{44,45} Finally, to improve the final analysis, the binding affinity ΔG (free energy change in kilocalories per mole (kcal/mol)) was calculated using PRODIGY.⁴⁶ A binding affinity threshold of -6.00 kcal/mol was used for PRODIGY to assess the stability and thermodynamic favorability of the protein-ligand complexes. This second approach adds a further degree of understanding to the thermodynamic perspective of protein-ligand complexes, revealing details of the stability and energetics of the formed complexes. Molecular docking, which incorporates conformational flexibility of the ligand and receptor, is a powerful technique that provides detailed mechanistic insights into the binding affinities of molecular details of atomic interactions.^{41,47} Lidocaine was used as the standard positive control for sodium channels to quantify inhibition as a surrogate readout for anesthetic activity. This allowed us to compare the activity profiles of bioactive secondary metabolites against a well-known anesthetic, thus creating a much clearer framework in which to consider them as potential novel anesthetic agents. All molecular docking simulations were conducted on a high-performance workstation equipped with an Intel® Core™ i7-12650H processor (16 cores, 2.30 GHz), NVIDIA™ RTX 4060 graphics card (8 GB VRAM), and 16 GB DDR5 RAM. This robust setup facilitated a thorough exploration of the potential binding modes and interactions between the selected bioactive secondary metabolites and human sodium channels. The use of AlphaFold to model the Nav1.9 structure, while innovative, introduces potential limitations due to the model's reliance on predicted rather than experimentally verified data, which may affect the accuracy of the docking results. The detailed insights gained from these simulations are crucial for the development of novel anesthetic agents targeting painful human dental pulps.

Computational ADME parameter prediction

To comprehensively assess the potential of the ligands to inhibit human sodium channels, a comprehensive examination of their toxicological features and oral bioavailability was conducted using the SwissADME tool (<http://www.swissadme.ch/>).⁴⁸ This advanced computational tool provides a comprehensive evaluation of the pharmacokinetic properties of ligands, including important parameters, such as ADME. SwissADME provides insights into the identification of ligands with better pharmacokinetic properties, informing the selection of candidates for further experimental validation. The evaluation of ADME parameters is pivotal in drug design and development as it provides insights into how the compound is absorbed, distributed, metabolized, and eliminated throughout the body.⁴⁹ Ligands with optimal ADME characteristics are more likely to exhibit desirable pharmacological effects and reduced toxicity, making them promising candidates for further preclinical and clinical studies.^{50,51} Through the utilization of SwissADME, this study ensured meticulous evaluation of the pharmacokinetic properties of each ligand, contributing to the overall understanding of their potential as anesthetic agents targeting human sodium channels.

Examination of drug-likeness and toxicity

In addition to ADME parameter prediction, a comprehensive assessment of drug-likeness and toxicity was conducted for all selected ligands using the OSIRIS DataWarrior V6.1.0.⁵² This in-depth analysis covered a broad spectrum of toxicities including tumorigenicity, mutagenicity, irritancy, and reproductive effects. By scrutinizing these toxicity endpoints, this study aimed to identify any potential adverse effects associated with these ligands and ensure a thorough evaluation of their safety profiles. Furthermore, the assessment encompassed the criteria for drug-likeness, which evaluates various molecular properties to determine the suitability of a compound for drug development. Factors such as molecular size, lipophilicity, hydrogen bonding potential, and structural alerts were considered to ascertain whether the ligands possessed characteristics conducive to drug-like properties.⁵³ This evaluative approach guarantees that the chosen ligands have pharmacological activity and satisfy critical parameters for generating successful drug candidates, whereas a computer-based multi-sided analysis of both drug-likeness and toxicity ensures that the ligands that best survive this filtering analysis advance to the next stage of evaluation, thereby improving the success of drug discovery.^{54,55} Combining these broad tests can help identify leads for new anesthetic agents that specifically target human sodium channels, while ensuring that they are safe and effective.

Pharmacophore modeling to assess active functional groups of bioactive secondary metabolites

Pharmacophore modeling is a cornerstone for deciphering intricate molecular interactions between ligands and their target receptors. Identifying and characterizing essential steric attributes, collectively termed pharmacophores, are crucial for the optimal binding and modulation of biological responses.^{31,56} In this study, we assessed the pharmacophore profile of ligands within the active pocket of the sodium channel receptors Nav1.7, Nav1.8, and Nav1.9. This process is essential for gaining insights into the specific functional groups and spatial arrangements required to effectively inhibit these channels. To ensure the validity and reliability of our pharmacophore model, we referred to a previous study for validation.⁵⁷ This involved comparing our model with established data and experimental results to confirm its accuracy in representing the essential features necessary for ligand binding and activity. Once rigorously validated, a 3D pharmacophore model is a powerful ligand-screening and selection tool. The pharmacophore-based screening process was executed using advanced algorithms within LigandScout 4.5,⁵⁸ a state-of-the-art molecular modeling and drug discovery software platform. This methodological approach enabled us to systematically analyze and prioritize ligands based on their pharmacophoric characteristics, such as hydrogen-bonding donors and acceptors, aromatic rings, and hydrophobic regions.⁵⁹ Focusing on these key molecular features, we aimed to identify compounds with the highest potential for therapeutic relevance as novel anesthetic agents for painful human dental pulp.

Results

Data selection and ligand structure development of bioactive secondary metabolites

The bioactive secondary metabolites of plants exhibiting anesthetic activities were screened by selecting medicinal plants for their traditional use and documented pharmacological activities, which were sorted according to their secondary metabolites, including essential oils, terpenoids, alkaloids, flavonoids, and stilbenoids. The selection criteria included plants with a significant history of use in traditional medicine, promising preclinical or clinical studies on compounds isolated from plants, and the identification of their bioactive secondary metabolites. All anesthetic actions were recorded and studied using various experimental models (Table 1).

They are divided into essential oils, terpenoids, alkaloids, flavonoids, and stilbenoids. Essential oils and terpenoids from peppermint (*Mentha piperita*), lavender (*Lavandula angustifolia*), marjoram (*Origanum majorana*), anise (*Pimpinella anisum*), myrrh (*Commiphora molmol*), and

clove (*Syzygium aromaticum*) have significant anesthetic effects. These included plants such as menthol, camphor, linalool, α -terpineol, anethole, furanodiene, methoxyfuranoguaia-9-ene-8-one, and β -caryophyllene, which were found to reduce electrically evoked contractions of rat phrenic nerve-hemidiaphragm preparations and increase the number of stimuli required to evoke the rabbit conjunctival reflex. These findings were corroborated by other experimental models, which suggested that essential oils and terpenoids have aesthetic properties.^{60–66} In addition to the anesthetic power of alkaloids and flavonoids/stilbenoids, the study showed that monkshood (*Aconitum* spp.) and larkspur (*Delphinium* spp.) contain powerful alkaloids, including aconitine, lappaconitine, bulleyaconitine A, sepaconitine, ranaconitine, and sarcorine. These alkaloids have a longer duration of anesthesia than conventional agents.^{67–69} Quinine from the Cinchona tree (*Cinchona* spp.) inhibits the K⁺/H⁺ exchanger in respiring mitochondria, emphasizing its anesthetic capabilities.⁷⁰ Flavonoids and stilbenoids from red wine (*Vitis* spp.), green tea (*Camellia sinensis*), bitter kola (*Garcinia kola*), and Japanese knotweed (*Fallopia japonica*) displayed potent inhibition of VGSC, VGK and VGCC, quercetin, catechin, rutin, epicatechin, anthocyanins, epigallocatechin-3-gallate, epigallocatechin, and resveratrol have proven to be promising.^{71–74} These findings highlight the potential of these natural compounds as effective anesthetics with varying degrees of efficacy and mechanisms of action, offering valuable insights for medical and pharmacological applications.

Molecular docking simulation

Docking simulations were performed to evaluate the binding affinities of the bioactive secondary metabolites to the ligand-binding domains (LBD) of Nav1.7, Nav1.8, and Nav1.9 sodium channels. These binding affinity values indicate the energies required for dissociation of the ligand from the protein receptor, offering insights into the stability of the complex as well as the binding affinity of the inhibitor, which is essential for designing compounds as inhibitors. Lidocaine, the clinically used anesthetic, was employed as a standard inhibitor to benchmark the performance of the bioactive secondary metabolites in terms of their inhibitory potencies (Table 2). This comparison helps evaluate the practical relevance of the identified compounds as potential alternatives or improvements over current anesthetics.

Molecular docking simulation results for the first five best-performing bioactive secondary metabolites were compared with lidocaine, the inhibitory standard for binding affinity to Nav1.7, Nav1.8, and Nav1.9 sodium channels (Table 3). For Nav1.7, sepaconitine demonstrated the highest HADDOCK performance score (−38.2) and the lowest binding affinity ($\Delta G = -8.95$ kcal/mol), significantly outperforming lidocaine (HADDOCK score = −29.9; $\Delta G = -7.20$ kcal/mol). The much lower dissociation constant ($K_d = 0.000388 \mu\text{M}$) indicated a

Table 2. (continued)

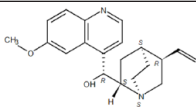
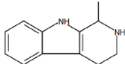
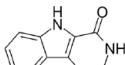
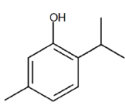
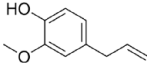
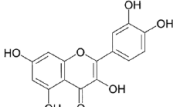
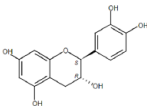
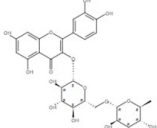
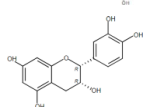
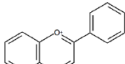
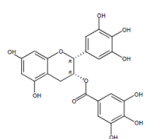
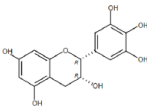
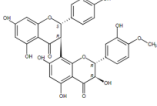
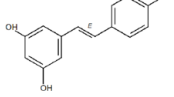
Bioactive secondary metabolite	Chemical structure	ΔG (kcal/mol)		
		Navl.7	Navl.8	Navl.9
Quinine ($C_{20}H_{24}N_2O_2$)		-7.65	-7.09	-6.90
Tetrahydroharman ($C_{12}H_{14}N_2$)		-7.38	-6.64	-6.16
Tetrahydronorharman ($C_{17}H_{20}N_2O_4$)		-6.55	-7.68	-7.63
Thymol ($C_{10}H_{14}O$)		-6.22	-5.90	-6.01
Eugenol ($C_{10}H_{12}O_2$)		-6.24	-5.90	-5.89
Quercetin ($C_{15}H_{10}O_7$)		-6.29	-7.06	-6.45
Catechin ($C_{15}H_{14}O_6$)		-6.64	-6.34	-6.43
Rutin ($C_{27}H_{30}O_{16}$)		-6.76	-7.86	-7.08
Epicatechin ($C_{15}H_{14}O_6$)		-6.22	-6.27	-6.27
Anthocyanins ($C_{15}H_{11}O$)		-6.37	-6.28	-6.36
Epigallocatechin-3-gallate ($C_{22}H_{18}O_{11}$)		-6.50	-7.10	-7.41
Epigallocatechin ($C_{15}H_{14}O_7$)		-6.22	-6.36	-6.34
Kolaflavanone ($C_{31}H_{24}O_{12}$)		-7.06	-7.78	-7.43
Resveratrol ($C_{14}H_{12}O_3$)		-6.68	-6.26	-6.30

Table 3. Comparative molecular docking analysis of bioactive secondary metabolites against Nav1.7, Nav1.8, and Nav1.9 sodium channel complexes, with lidocaine as a reference inhibitor.

Complex	HADDOCK score	Binding affinity ΔG (kcal/mol)	Kd (μM)	Cluster size	RMSD	Van der Waals energy	Electrostatic energy	Desolvation energy	Restraints violation energy
Nav1.7 complexes									
Nav1.7:Lidocaine (Standard inhibitor)	-29.9 ± 0.3	-7.20	0.61	6	0.2 ± 0.2	-14.3 ± 0.3	-90.7 ± 1.7	-6.6 ± 0.1	0.0 ± 0.1
Nav1.7:Sepaconitine	-38.2 ± 3.1	-8.95	0.000388	4	0.4 ± 0.2	-20.4 ± 1.9	-117.1 ± 14.1	-6.2 ± 0.3	0.0 ± 0.0
Nav1.7:Lappaconitine	-32.9 ± 1.2	-7.77	0.12	6	0.9 ± 0.1	-20.1 ± 0.7	-46.8 ± 9.5	-8.2 ± 0.6	0.2 ± 0.1
Nav1.7:Aconitine	-32.7 ± 0.4	-7.72	0.14	17	0.7 ± 0.1	-19.3 ± 0.7	-48.0 ± 15.1	-8.7 ± 1.3	0.6 ± 0.7
Nav1.7:Quinine	-34.0 ± 0.2	-7.65	0.17	8	1.7 ± 0.0	-17.1 ± 0.4	-111.9 ± 1.8	-5.7 ± 0.3	0.0 ± 0.0
Nav1.7:Ranaconitine	-28.4 ± 0.3	-7.44	0.38	33	0.8 ± 0.0	-18.0 ± 0.4	-63.6 ± 2.9	-4.0 ± 0.3	0.0 ± 0.0
Nav1.8 complexes									
Nav1.8:Lidocaine (Standard inhibitor)	-20.0 ± 0.1	-6.76	6.80	5	0.8 ± 0.1	-12.2 ± 0.2	-85.1 ± 0.7	0.4 ± 0.1	2.4 ± 0.3
Nav1.8:Lappaconitine	-32.0 ± 0.1	-8.00	0.02	59	0.3 ± 0.2	-24.9 ± 0.5	-98.4 ± 3.0	2.4 ± 0.1	2.9 ± 1.3
Nav1.8:Rutin	-27.5 ± 0.9	-7.86	0.07	24	0.5 ± 0.0	-24.1 ± 1.1	-92.1 ± 3.5	5.7 ± 0.2	2.1 ± 0.6
Nav1.8:Kolafavanone	-27.6 ± 0.4	-7.78	0.12	6	0.3 ± 0.2	-23.8 ± 0.6	-74.1 ± 3.7	3.2 ± 0.4	3.5 ± 0.8
Nav1.8:Sepaconitine	-27.7 ± 0.2	-7.73	0.13	31	0.5 ± 0.0	-19.2 ± 0.4	-114.4 ± 1.7	2.7 ± 0.2	2.4 ± 0.5
Nav1.8:Tetrahydronorharman	-31.4 ± 0.4	-7.68	0.15	20	0.1 ± 0.1	-17.6 ± 0.4	-146.3 ± 2.1	0.6 ± 0.2	2.6 ± 1.0
Nav1.9 complexes									
Nav1.9:Lidocaine (Standard inhibitor)	-19.7 ± 1.3	-6.41	30.20	7	1.5 ± 0.0	-13.9 ± 1.1	-24.6 ± 4.3	-3.7 ± 0.3	3.8 ± 0.2
Nav1.9:Ranaconitine	-12.6 ± 1.9	-8.03	2.15	5	1.7 ± 0.0	-25.8 ± 2.2	6.4 ± 3.4	-2.6 ± 0.5	150.5 ± 2.3
Nav1.9:Sepaconitine	-6.9 ± 2.5	-7.92	2.56	4	1.0 ± 0.0	-22.7 ± 0.4	-7.9 ± 0.2	-0.3 ± 0.1	169.0 ± 19.6
Nav1.9:Lappaconitine	-32.5 ± 1.5	-7.71	3.63	4	1.8 ± 0.0	-26.4 ± 1.0	-27.3 ± 11.0	-3.9 ± 0.3	4.9 ± 0.9
Nav1.9:Tetrahydronorharman	-13.1 ± 1.6	-7.63	4.18	5	1.9 ± 0.0	-18.1 ± 0.7	-74.9 ± 10.0	-2.4 ± 0.2	149.2 ± 0.3
Nav1.9:Kolafavanone	-16.9 ± 1.4	-7.43	5.71	4	1.8 ± 0.0	-19.1 ± 0.7	-9.0 ± 6.2	2.5 ± 0.3	5.2 ± 1.2

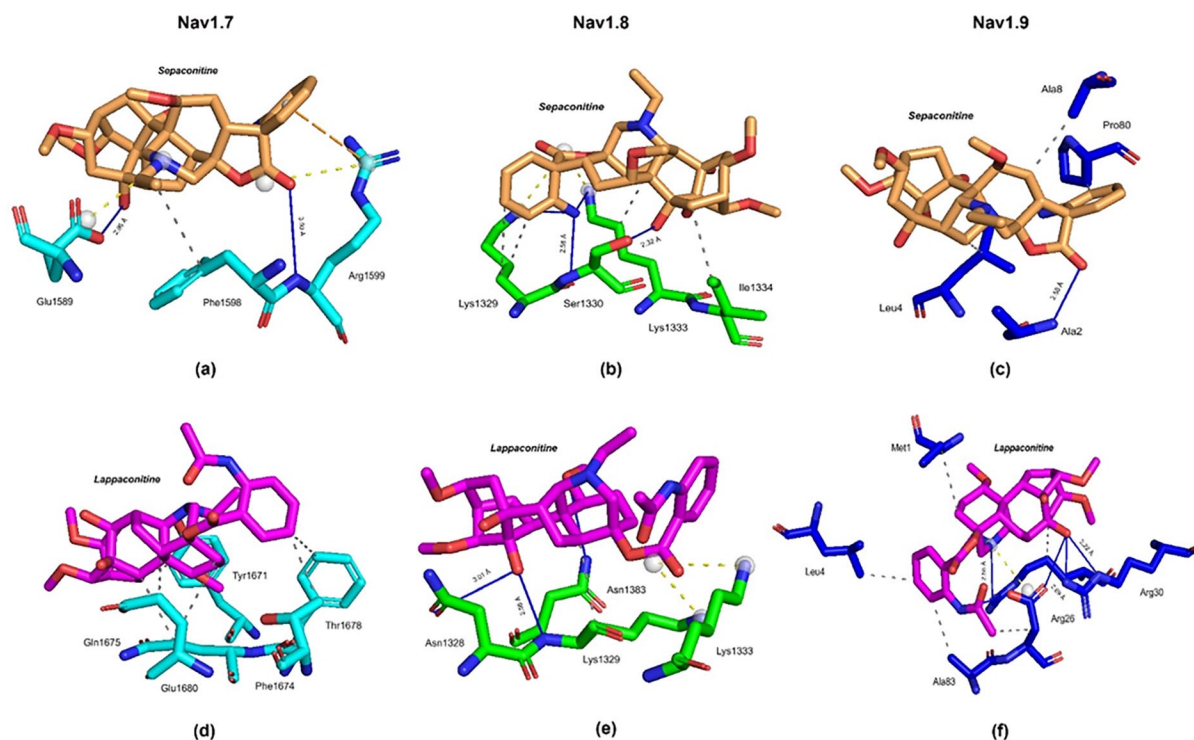


Figure 1. 3D visualization: Binding pose of Sepaconitine and Lappaconitine (as ligands exhibiting consistently high binding affinities and stability) across Nav1.7, Nav1.8, and Nav1.9 channels. (a) Sepaconitine binding to Nav1.7. (b) Sepaconitine binding to Nav1.8. (c) Binding to Nav1.9. (d) Lappaconitine binding to Nav1.7. (e) Binding to the Nav1.8. (f) Binding to the Nav1.9. Blue lines represent the hydrogen bonds, while dotted lines depict hydrophobic interactions.

stronger interaction between Sepaconitine and Nav1.7, suggesting its potential to be a very efficient inhibitor. In comparison, lidocaine, with a K_d of $0.025\mu\text{M}$, exhibited a much weaker interaction, highlighting the superior potency of Sepaconitine. Aconitine also showed relatively high binding affinity (-7.77kcal/mol) and a stable HADDOCK score of -32.9 , though it was slightly less effective than Sepaconitine. Quinine, and Ranaconitine, with binding affinities of -7.65kcal/mol and -7.44kcal/mol , respectively, outperformed lidocaine, with quinine in particular showing a promising HADDOCK score of -34.0 , suggesting a substantial van der Waals energy contribution of -17.1kcal/mol , which could enhance its potential as a Nav1.7 inhibitor. Ranaconitine, despite a lower HADDOCK score (-28.4), still surpassed lidocaine in terms of binding affinity, suggesting a moderate yet significant efficacy.

For Nav1.8, lappaconitine stood out with a HADDOCK score of -32.0 and a binding affinity of -8.00kcal/mol , significantly surpassing lidocaine's HADDOCK score of -20.0 and binding affinity of -6.76kcal/mol , suggesting a much stronger and more stable interaction. This demonstrates that lappaconitine could be a more effective inhibitor than lidocaine for Nav1.8 inhibition. Rutin (binding affinity $= -7.86\text{kcal/mol}$) and Kolaflavanone (binding affinity $= -7.78\text{kcal/mol}$) also showed promising results, with favorable HADDOCK scores of -27.5

and -27.6 , respectively. Sepaconitine, with a binding affinity of -7.73kcal/mol , showed consistent efficacy across different sodium channels, exhibiting binding affinities of -7.70kcal/mol at Nav1.2, -7.73kcal/mol at Nav1.7, and -7.73kcal/mol at Nav1.8, positioning it as a potential broad-spectrum inhibitor. Tetrahydronorharman demonstrated moderate inhibitory performance with a binding affinity of -7.68kcal/mol , outperforming the reference inhibitor, Saingamide (binding affinity $= -6.83\text{kcal/mol}$). The HADDOCK score of -31.4 indicated a strong interaction between Tetrahydronorharman and Nav1.8, suggesting it could be a viable alternative to lidocaine. 3D and 2D representations of ligand and receptor binding pose are shown in Figures 1 and 2 respectively, demonstrated a clear view of their interaction.

For Nav1.9, lidocaine exhibited a binding affinity of -6.41kcal/mol and a HADDOCK score of -19.7 , setting the benchmark for comparison. Lappaconitine emerged as the most effective inhibitor with a binding affinity of -7.71kcal/mol and a HADDOCK score of -32.5 , indicating a very strong and stable interaction, suggesting it could potentially be more effective than lidocaine for Nav1.9 inhibition. Sepaconitine, with binding affinities of -8.03kcal/mol and -7.92kcal/mol , also outperformed lidocaine. However, their higher dissociation constants (K_d) suggested slightly less stable interactions compared to their performance with

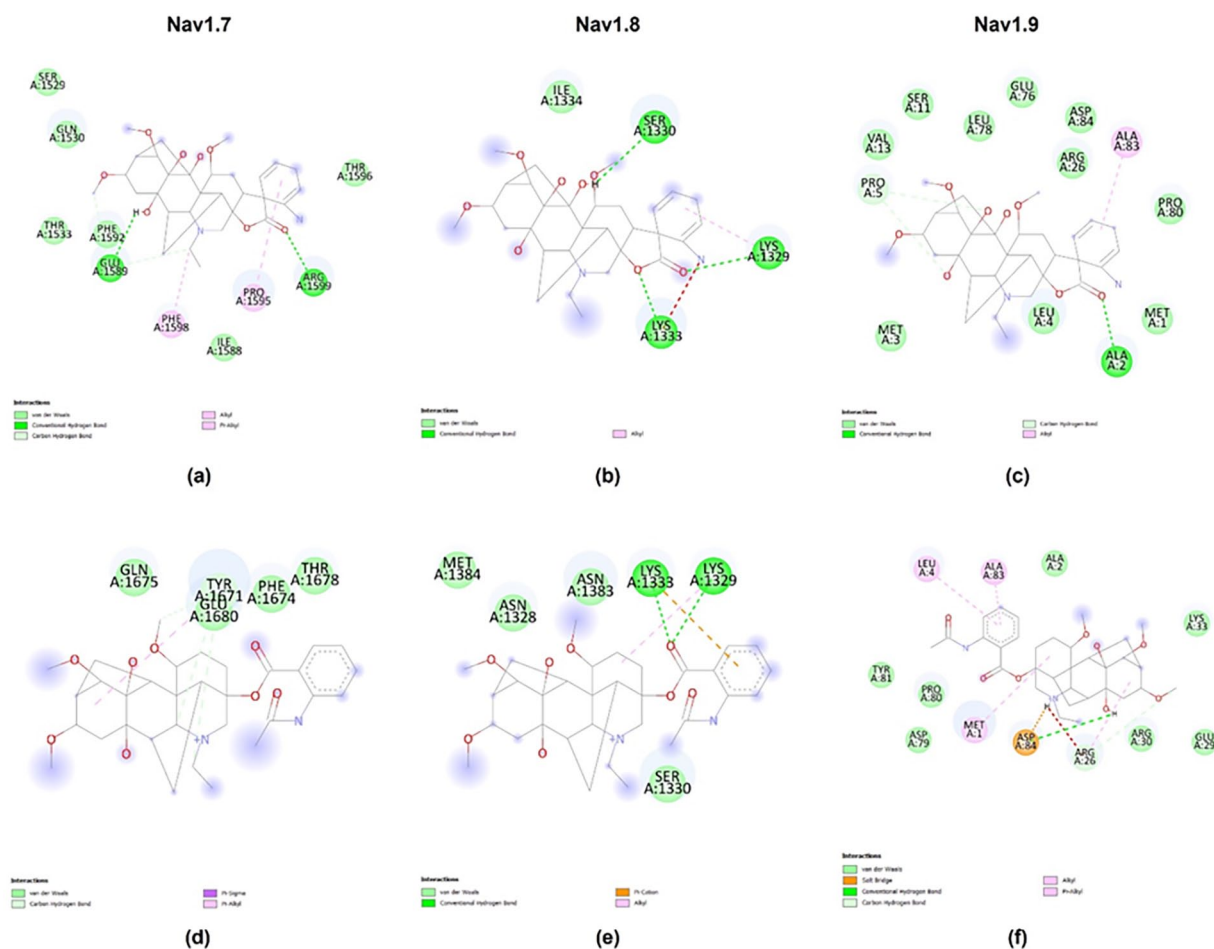


Figure 2. 2D visualization: Binding pose of Sepaconitine and Lappaconitine (as ligands exhibiting consistently high binding affinities and stability) across Nav1.7, Nav1.8, and Nav1.9 channels. (a) Sepaconitine binding to Nav1.7. (b) Sepaconitine binding to Nav1.8. (c) Binding to Nav1.9. (d) Lappaconitine binding to Nav1.7. (e) Binding to the Nav1.8. (f) Binding to the Nav1.9.

The ligand-receptor interactions are visualized with distinct color coding to represent various types of interactions. Classic hydrogen bonds are depicted in green, carbon-hydrogen bonds in turquoise, van der Waals interactions in light green, π -alkyl interactions in pink, and π -sigma interactions in purple. This color scheme aids in distinguishing between the different non-covalent interactions that contribute to the stability and specificity of the ligand-receptor binding.

Nav1.7 and Nav1.8. These compounds had HADDOCK scores of -12.6 and -6.9 , showing varied performance. Tetrahydronorharman and Kolaflavanone, with binding affinities of -7.63 kcal/mol and -7.43 kcal/mol, respectively, showed moderate effectiveness but were still superior to lidocaine. Their HADDOCK scores of -13.1 and -16.9 indicated reasonable interaction stability. Energy contributions to the binding interactions reveal more about the potency of these compounds. For Nav1.7, the van der Waals energy (which contributes to hydrophobic interactions, a major driving force for binding interactions) was highest for Sepaconitine (-20.4 kcal/mol), and its electrostatic energy (-117.1 kcal/mol) also showed the highest value, suggesting a highly favorable binding profile. Lappaconitine and Aconitine showed strong van der Waals and electrostatic energy contributions, indicating stable and robust interactions with Nav1.7. Inconsistent with their high binding

affinities, van der Waals and electrostatic energies were also strong for Lappaconitine and Aconitine, suggesting stable interactions with Nav1.7. For Nav1.8, Lappaconitine exhibited strong van der Waals energy (-24.9 kcal/mol) and electrostatic energy (-98.4 kcal/mol), further supporting its effectiveness. For Nav1.9, the energy contributions (van der Waals: -26.4 kcal/mol, electrostatic: -27.3 kcal/mol) were highest for Lappaconitine, confirming its superior binding profile and robust interaction. Sepaconitine and Lappaconitine exhibited superior binding affinities and robustness against Nav1.7, Nav1.8, and Nav1.9 channels compared to lidocaine. These compounds, driven by high van der Waals and electrostatic interactions, suggest they could be potent sodium channel blockers and offer a rationale for their development as alternatives to lidocaine. These findings demonstrate that these bioactive secondary metabolites could be excellent candidates for further development into new

anesthetic drugs, potentially addressing unmet needs in the anesthetic drug market, as shown in Supplementary Data 1.

Computational ADME parameter prediction

Computational ADME properties and Cytochrome P450 (CYP) inhibition profiles offer crucial insights into the pharmacokinetic characteristics and potential metabolic interactions of bioactive secondary metabolites. These properties are essential considerations in drug development to ensure adequate bioavailability, distribution, metabolism, and elimination, thereby influencing the efficacy and safety of the therapeutic agents. Table 4 shows the predicted ADME parameters and CYP-inhibitory activities of the selected bioactive secondary metabolites. Photocredit: Aconitum-derived natural products, namely Sepaconitine, Lappaconitine, Aconitine, and Ranaconitine, demonstrated favorable binding affinity toward Nav1.7, Nav1.8, and Nav1.9 sodium channel complexes. However, the ADME profiles of these compounds exhibited some interesting features. Sepaconitine, for instance, possesses favorable ADME features with MW (558.66 g/mol), low lipophilicity (MlogP=0.54) and moderate number of HBA and HBD. These features indicate that it would have moderate absorption and distribution potential while lowering its liabilities to undergo metabolic clearance. Nonetheless, the inhibition of CYP2D6 by Sepaconitine raises concerns that these drugs may cause drug-drug interactions, and therefore, extraordinary caution should be used in any therapeutic application.

Despite its strong binding affinity, lappaconitine exhibits Lipinski violation and CYP2D6 inhibition. This violation, along with its MW of 584.70 g/mol and relatively high TPSA (Topological Polar Surface Area) of 126.79 Å², may impact its bioavailability and distribution. Moreover, its interaction with CYP2D6 suggests potential metabolic interactions, emphasizing the need for cautious dosing strategies and monitoring. Aconitine and Ranaconitine exhibited good binding affinity for Na⁺ channels but exhibited poor ADME profiles. Aconitine has a high MW (645.74 g/mol), a high count of HBA and HBD, which may hinder gut absorption and distribution. It interacts with various CYP isoforms, indicating multimodal metabolism of the compound, which necessitates detailed pharmacokinetic studies. Ranaconitine (600.70 g/mol and relatively high TPSA (from an absorption and distribution standpoint) exhibit similar effects as its inhibition of CYP2D6, which can determine the metabolic fate of the drug and could potentially result in drug-drug interactions that alter the safety and efficacy profile of the compound. Conversely, rutin, a flavonoid glycoside, provided greater favorable ADME profiling, namely a MW of 610.52 g/mol and low lipophilicity, as well as limited CYP inhibition. These properties indicate a higher potential for bioavailability and pharmacokinetic distribution, although its large number of TPSA and Lipinski violations may still present challenges. Thus, although the assessed bioactive

secondary metabolites are good scaffolds for future pain-relief drugs, their ADME parameters also show the need for greater appreciation of pharmacokinetic properties alongside binding affinities.

Examination of drug-likeness and toxicity

A focused study on profiling the drug-likeness and toxicity of bioactive secondary metabolites will help predict their therapeutic utility and potential toxicity. As shown in Table 5, many compounds have different toxicity and drug-likeness profiles; therefore, we can predict that some compounds might be suitable for therapeutic use. Although menthol and camphor scored highly for mutagenicity, tumorigenicity, and irritancy, for which they have been known for a while to be highly toxic, they have high efficacy, suggesting that they have potent pharmacological activity. However, such high toxicity suggests that they are not safe or well-tolerated in therapeutic regimes. Similarly, despite a high efficacy score and high toxicity score, the latter means that careful assessment is required because although it could prove to be a useful pharmacologically active component, it might not be safe.

In contrast, compounds such as linalool, α -terpineol, and β -caryophyllene showed fewer toxicological concerns with relatively neutral drug-likeness scores. While Linalool is non-reproductive but is associated with high irritancy, α -terpineol and β -caryophyllene present relatively favorable safety profiles, making them potentially attractive candidates for further investigation. Aconitine, Lappaconitine, Bulleyaconitine A, Sepaconitine, and Ranaconitine demonstrated moderate drug-likeness scores, suggesting their potential for use as drug candidates. However, their moderate to high toxicity profiles raise safety concerns, necessitating the comprehensive evaluation and development of mitigation strategies to minimize adverse effects. Tetrahydroharman exhibits low mutagenicity and moderate drug-likeness, indicating a relatively favorable safety profile compared to other compounds. Conversely, Tetrahydronorharman displays significantly negative drug-likeness, raising questions about its pharmacological applicability despite its relatively neutral toxicity profile. Compounds such as Thymol, Eugenol, and Quercetin demonstrate high mutagenicity and irritant properties, limiting their therapeutic utility, despite their moderate drug-likeness scores. Rutin, Catechin, Epicatechin, Anthocyanins, Epigallocatechin-3-gallate, and Epigallocatechin exhibited moderate to low drug-likeness with minimal toxicological concerns, suggesting potential pharmacological activity that warrants further investigation. Despite its moderate drug-likeness, kolaflavanone is associated with high reproductive toxicity, underscoring the importance of evaluating both its efficacy and safety profiles in drug development. Finally, despite its moderate drug-likeness, resveratrol exhibits high mutagenicity and irritancy, indicating potential limitations that must be addressed for its therapeutic use.

Table 4. Computational ADME properties and CYP inhibition of bioactive secondary metabolites.

Bioactive secondary metabolite	MW (g/mol)	MlogP	HBA	HBD	TPSA (Å ²)	Lipinski violation	CYP inhibitor
Menthol (C ₁₀ H ₂₀ O)	156.27	2.45	1	1	20.23	0	None
Camphor (C ₁₀ H ₁₆ O)	152.23	2.30	1	0	17.07	0	None
Linalool (C ₁₀ H ₁₈ O)	154.25	2.59	1	1	20.23	0	None
α-Terpineol (C ₁₀ H ₁₈ O)	154.25	2.30	1	1	20.23	0	None
Anethole (C ₁₀ H ₁₂ O)	148.20	2.67	1	0	9.23	0	CYP1A2
Furanodiene (C ₁₅ H ₂₀ O)	216.32	3.33	1	0	13.14	0	None
Methoxyfuranoguaia-9-ene-8-one (C ₁₆ H ₂₀ O ₃)	260.33	1.77	3	0	39.44	0	None
β-Caryophyllene (C ₁₅ H ₂₄)	204.35	4.63	0	0	0.00	1	CYP2C19, CYP2C9
Aconitine (C ₃₄ H ₄₇ NO ₁₁)	645.74	0.23	12	3	153.45	2	None
Lappaconitine (C ₃₂ H ₄₄ N ₂ O ₈)	584.70	1.24	9	3	126.79	1	CYP2D6
Bulleyaconitine A (C ₃₅ H ₄₉ NO ₉)	627.76	1.12	10	1	112.99	1	CYP2C19
Sepaconitine (C ₃₀ H ₄₂ N ₂ O ₈)	558.66	0.54	9	4	143.94	1	CYP2D6
Ranaconitine (C ₃₂ H ₄₄ N ₂ O ₉)	600.70	0.48	10	4	147.02	2	CYP2D6
Sarcorine (C ₂₅ H ₄₄ N ₂ O)	388.63	4.14	2	1	32.34	0	None
Quinine (C ₂₀ H ₂₄ N ₂ O ₂)	324.42	2.23	4	1	45.59	0	CYP2D6
Tetrahydroharman (C ₁₂ H ₁₄ N ₂)	186.25	1.84	1	2	27.82	0	CYP1A2, CYP2D6
Tetrahydronorharman (C ₁₇ H ₂₀ N ₂ O ₄)	316.35	1.61	4	2	82.63	0	None
Thymol (C ₁₀ H ₁₄ O)	150.22	2.76	1	1	20.23	0	CYP1A2
Eugenol (C ₁₀ H ₁₂ O ₂)	164.20	2.01	2	1	29.46	0	CYP1A2
Quercetin (C ₁₅ H ₁₀ O ₇)	302.24	-0.56	7	5	131.36	0	CYP1A2, CYP2D6, CYP3A4
Catechin (C ₁₅ H ₁₄ O ₆)	290.27	0.24	6	5	110.38	0	None
Rutin (C ₂₇ H ₃₀ O ₁₆)	610.52	-3.89	16	10	269.43	3	None
Epicatechin (C ₁₅ H ₁₄ O ₆)	290.27	0.24	6	5	110.38	0	None
Anthocyanins (C ₁₅ H ₁₁ O)	207.25	3.28	1	0	13.14	0	CYP1A2, CYP2D6
Epigallocatechin-3-gallate (C ₂₂ H ₁₈ O ₁₁)	458.37	-0.44	11	8	197.37	2	None
Epigallocatechin (C ₁₅ H ₁₄ O ₇)	306.27	-0.29	7	6	130.61	1	None
Kolaflavanone (C ₃₁ H ₂₄ O ₁₂)	588.52	-0.48	12	7	203.44	3	CYP2C9, CYP3A4
Resveratrol (C ₁₄ H ₁₂ O ₃)	228.24	2.26	3	3	60.69	0	CYP1A2, CYP2C9, CYP3A4

In our comprehensive evaluation of bioactive secondary metabolites, three compounds emerged as top candidates for inhibiting neuropathic pain through modulation of Nav1.7, Nav1.8, and Nav1.9 receptors (Table 6). Sepaconitine, Lappaconitine, and Ranaconitine demonstrated robust binding affinities across all three receptor subtypes, indicating their potential efficacy in pain attenuation. Sepaconitine, which has notable ΔG values across all the receptors, is a promising candidate. Its strong binding affinity suggests an effective interaction with the target receptors, making it a compelling option for further investigation. Similarly, Lappaconitine exhibited consistent binding performance, indicating its potential as a versatile inhibitor across Nav1.7, Nav1.8, and Nav1.9 channels. Ranaconitine was less potent than Sepaconitine and Lappaconitine but still bound well to all three receptor types. Its profile suggests a role in neuropathic pain and warrants further investigation of its therapeutic potential. Moreover, these selected metabolites possess desirable ADME properties, including good bioavailability and favorable metabolic stability. Additionally,

their drug-likeness scores implied compatibility with the drug development criteria, suggesting the feasibility of further preclinical and clinical investigations. Furthermore, the absence of toxicity concerns enhanced the attractiveness of these compounds for therapeutic applications. These low values indicate that they are unlikely to be mutagenic, carcinogenic, or irritant, which is a desirable feature for potential new pharmaceutical agents.

Pharmacophore modeling to assess active functional groups of bioactive secondary metabolites

Among the top three ligands, Sepaconitine, Lappaconitine, and Ranaconitine were subjected to detailed pharmacophore modeling to establish the features of the active moieties that produced the binding pattern to the three Nav channels (Nav1.7, Nav1.8, and Nav1.9) by adopting specific conformations and interactions. The results obtained from 2D and 3D pharmacophore tests offer valuable insights into the

Table 5. Toxicological profiles and drug-likeness of bioactive secondary metabolites.

Bioactive secondary metabolite	Drug-likeness	Mutagenic	Tumorigenic	Reproductive effective	Irritant
Menthol (C ₁₀ H ₂₀ O)	-10.47	High	High	None	High
Camphor (C ₁₀ H ₁₆ O)	-3.71	High	High	High	High
Linalool (C ₁₀ H ₁₈ O)	-6.68	None	None	None	High
α -Terpineol (C ₁₀ H ₁₈ O)	-3.35	None	None	None	Low
Anethole (C ₁₀ H ₁₂ O)	-4.04	High	High	High	None
Furanodiene (C ₁₅ H ₂₀ O)	-2.20	None	None	None	None
Methoxyfuranoguaia-9-ene-8-one (C ₁₆ H ₂₀ O ₃)	0.08	None	None	None	None
β -Caryophyllene (C ₁₅ H ₂₄)	-6.47	None	None	None	None
Aconitine (C ₃₄ H ₄₇ NO ₁₁)	4.92	None	None	None	None
Lappaconitine (C ₃₂ H ₄₄ N ₂ O ₈)	4.60	None	None	None	None
Bulleyaconitine A (C ₃₅ H ₄₉ NO ₉)	4.27	None	None	None	None
Sepaconitine (C ₃₀ H ₄₂ N ₂ O ₈)	3.65	None	None	None	None
Ranaconitine (C ₃₂ H ₄₄ N ₂ O ₉)	4.68	None	None	None	None
Sarcorine (C ₂₅ H ₄₄ N ₂ O)	3.04	None	None	None	None
Quinine (C ₂₀ H ₂₄ N ₂ O ₂)	0.87	None	None	None	None
Tetrahydroharman (C ₁₂ H ₁₄ N ₂)	4.31	Low	None	None	None
Tetrahydronorharman (C ₁₇ H ₂₀ N ₂ O ₄)	-33.02	None	None	None	None
Thymol (C ₁₀ H ₁₄ O)	-2.33	High	None	High	None
Eugenol (C ₁₀ H ₁₂ O ₂)	-4.64	High	High	None	High
Quercetin (C ₁₅ H ₁₀ O ₇)	-0.08	High	High	None	None
Catechin (C ₁₅ H ₁₄ O ₆)	0.31	None	None	None	None
Rutin (C ₂₇ H ₃₀ O ₁₆)	1.93	None	None	None	None
Epicatechin (C ₁₅ H ₁₄ O ₆)	0.31	None	None	None	None
Anthocyanins (C ₁₅ H ₁₁ O)	-6.20	None	None	None	None
Epigallocatechin-3-gallate (C ₂₂ H ₁₈ O ₁₁)	-0.32	None	None	None	None
Epigallocatechin (C ₁₅ H ₁₄ O ₇)	0.31	None	None	None	None
Kolaflavanone (C ₃₁ H ₂₄ O ₁₂)	0.56	None	None	High	None
Resveratrol (C ₁₄ H ₁₂ O ₃)	-1.67	High	None	High	None

Table 6. The top three bioactive secondary metabolites (ligands) were selected based on the outcomes of molecular docking simulations, ADME parameters, drug-likeness, and toxicity assessments.

Bioactive secondary metabolite	ΔG (kcal/mol)			Drug-likeness	Toxicity
	Nav1.7	Nav1.8	Nav1.9		
Sepaconitine	-8.95	-7.73	-7.92	3.65	None
Lappaconitine	-7.77	-8.00	-7.71	4.60	None
Ranaconitine	-7.44	-7.51	-8.03	4.68	None

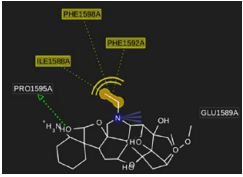
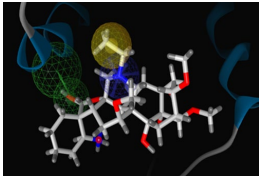
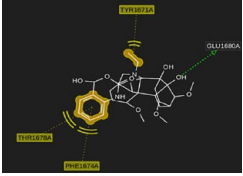
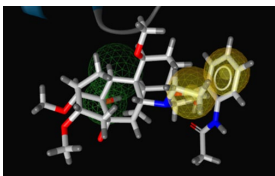
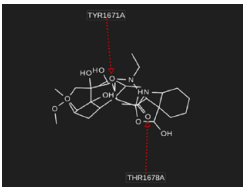
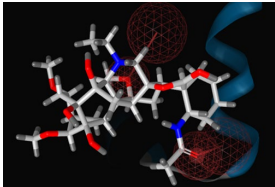
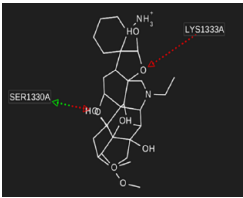
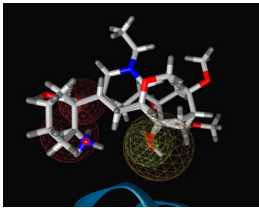
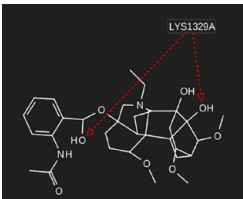
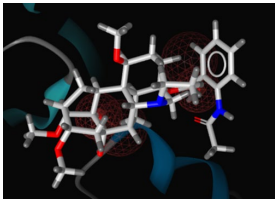
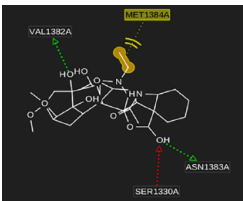
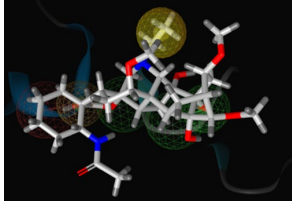
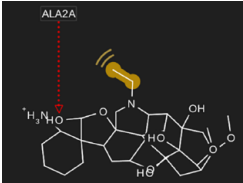
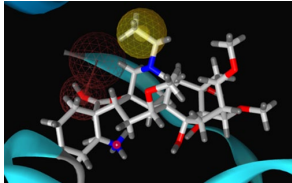
binding mechanism and stability of the binding of the three ligands (Sepaconitine, Lappaconitine, and Ranaconitine) to the three sodium channel subtypes (Nav1.7, Nav1.8, and Nav1.9) through several types of interactions. The outcomes of the 2D and 3D pharmacophore tests are summarized in Table 7.

Pharmacophore modeling of sepaconitine revealed that its amine group is crucial for hydrophobic interactions with specific residues on Nav1.7 and Nav1.9 receptors. In Nav1.7, the amine group interacts with Ile1588, Phe1592, and Phe1598, which are known to play roles in ligand binding and channel modulation. These interactions suggest that sepaconitine stabilizes the channel in a conformation that

enhances its binding affinity. For the Nav1.9 receptor, sepaconitine's amine group of sepaconitine interacts with the Ala2 residue, indicating a different binding site or mode compared with Nav1.7. This unique interaction highlights the versatility of ligands for adapting to various receptor environments. In contrast, sepaconitine binds to Nav1.8 primarily through hydrogen bonds formed by its carboxyl group with Ser1330 and Lys1333. These hydrogen bonds suggest that while the binding mode differs from that of Nav1.7 and Nav1.9, it still maintains a strong interaction, contributing to the overall efficacy of the ligand.

Lappaconitine has a pharmacophore profile in which its benzene ring primarily drives hydrophobic interactions with

Table 7. Pharmacophore models were developed using both 2D and 3D structural data, derived from the most favorable docking conformations.

Complex	2D pharmacophore	3D pharmacophore
NavI.7 complexes		
Sepaconitine:NavI.7		
Lappaconitine:NavI.7		
Ranaconitine:NavI.7		
NavI.8 complexes		
Sepaconitine:NavI.8		
Lappaconitine:NavI.8		
Ranaconitine:NavI.8		
NavI.9 complexes		
Sepaconitine:NavI.9		

(continued)

Table 7. (continued)

Complex	2D pharmacophore	3D pharmacophore
Lappaconitine:Nav1.9		
Ranaconitine:Nav1.9		

In the resulting visualizations, yellow spheres highlight regions of hydrophobic interactions, emphasizing areas where non-polar interactions play a crucial role in ligand binding. The green arrows represent hydrogen bond donors, indicating atoms that are capable of donating a hydrogen atom to form hydrogen bonds. Conversely, the red spheres identify hydrogen bond acceptors, marking atoms that can accept hydrogen bonds, thereby contributing to the stability and specificity of the ligand binding to the receptor.

Nav1.7 and Nav1.9. This is very important because this benzene ring interacts with residues Phe1674 and Thr1678 in Nav1.7, which are critical for maintaining the structural integrity of the channel and its function. This interaction suggests that lappaconitine may stabilize the receptor in a conformation favorable for binding. Similarly, on Nav1.9, lappaconitine's benzene ring engages Leu4 and Ala83, indicating a binding mode comparable to that observed on Nav1.7. Furthermore, convergence across subtypes points to the potential of the ligand as a pan-sodium channel modulator. For Nav1.8, hydrogen bonding remains the primary interaction mechanism; however, a different paradigm has been suggested. Since Nav1.8 has no hydrophobic interactions, differences in the nature of the receptor's binding pocket might necessitate alternative binding strategies to achieve both stability and efficacy.

Ranaconitine shows a distinctive pharmacophore profile when interacting with Nav1.8 and Nav1.9, where its amine group plays a pivotal role in hydrophobic interactions. In Nav1.8, the amine group interacts with Met1384, a residue that likely contributes to the ligand's strong binding affinity and stability. In Nav1.9, the amine group engages with Leu78, indicating a binding mechanism similar to that observed in Nav1.8. However, the interaction with Nav1.7 is markedly different. It acts primarily as a hydrogen bond acceptor, interacting with Tyr1671 and Thr1678. This shift in the interaction type suggests that ranaconitine can adapt its binding strategy to fit the specific structural characteristics of different sodium channel subtypes, highlighting its versatility as a ligand.

Discussion

In molecular docking simulations, Sepaconitine, Lappaconitine, and Ranaconitine also demonstrated high binding affinities for

Nav1.7, Nav1.8, and Nav1.9 sodium channels, respectively, thus describing Sepaconitine, Lappaconitine and Ranaconitine as potent inhibitors of sodium channels. These findings were further corroborated by a growing number of studies reporting that natural compounds can regulate the function of pain-associated ion channels. Sepaconitine had the highest affinity for Nav1.7, and was much more potent as an inhibitor of the binding site than the standard drug lidocaine. This alludes to significant inhibition with good contact with the binding site in the human channel and indicates potential efficacy as a painkiller by blocking pain signals. Previous studies have demonstrated the ability of aconitine derivatives to block sodium channels and manage neuropathic pain.^{75,76} The extremely high affinity of sepaconitine could be explained by its ability to form multiple hydrophobic interactions and hydrogen bonds with key residues (Ile1588, Phe1592, and Phe1598) on Nav1.7, thus stabilizing the ligand-receptor complex. All three compounds were very potent against Nav1.8 (which is involved in chronic pain conditions such as inflammatory pain, and effective inhibition of this channel can greatly alleviate pain symptoms.⁴ The very high affinity of lappaconitine suggests that it may be a selective Nav1.8 inhibitor in view of its high-affinity interactions with the important channel stability/function-related residues Ser1330 and Lys1333. Ranaconitine has a high affinity for Nav1.9, and is known to play a role in inflammatory and neuropathic pain,⁹ and its inhibition can provide significant therapeutic benefits. The binding affinity of ranaconitine to residues Leu78 and Ala83 was particularly strong and stable, providing further evidence for its potential drug-likeness. These data are in line with the existing literature, which suggests the analgesic potential of natural alkaloids from *Aconitum* species as sodium channel modulators.^{77,78} The ability of these compounds to stably interact with multiple sodium channel subtypes highlights

their versatility and potential for use in broad-spectrum pain management.

In addition, the ADME properties (pharmacokinetic characteristics) and therapeutic potential were evaluated. The ADME properties determine the bioavailability and systemic distribution of certain compounds. Therefore, these properties are directly proportional to the efficacy and safety of the compounds. Therefore, these properties are of great importance in determining the therapeutic potential of these compounds, as sepaconitine has good ADME properties and Moderate HBA and HBD activities. Therefore, it is advantageous in terms of absorption and distribution, as these two characteristics are prerequisites for good drug delivery.⁷⁹ However, Sepaconitine is also a CYP2D6 inhibitor, suggesting that it may be prone to drug-drug interactions, and thus requires more cautious clinical use. Another study highlighted CYP450 inhibition by natural products, which would likely require close monitoring and dosage adjustments.⁸⁰ Lappaconitine exhibited promising ADME characteristics despite violating Lipinski's rule of five, which could affect its bioavailability. Its molecular weight of 584.70 g/mol and relatively TPSA of 126.79 Å² suggest that while it may face challenges in crossing cell membranes, its strong binding affinity to sodium channels indicates it could still be effective with appropriate formulation strategies.⁸¹ CYP2D6 inhibition by lappaconitine further emphasized the importance of metabolic interactions in the therapeutic arena. Metabolic considerations may be particularly troublesome for ranaconitine, which possesses a high molecular weight, and TPSA, potentially complicating its pharmacokinetic profile. Nonetheless, its inhibition of multiple sodium channel subtypes makes it an intriguing agent for pain treatment, assuming that its pharmacokinetic profile could be optimized. Overall, we can conclude that the binding affinity, stability of the interaction with sodium channels, and pharmacokinetic profile should be optimized.⁸²

The toxicity and pharmacokinetic profiles of Sepaconitine, Lappaconitine, and Ranaconitine were thoroughly evaluated to ensure their safety and therapeutic potential. The results indicated that all three compounds exhibited low mutagenicity, tumorigenicity, and irritancy, suggesting that they possess relatively safe toxicity profiles for clinical use. These findings are particularly important for advancing these compounds as therapeutic agents. In fact, Sepaconitine showed no significant toxicity concerns, making it an appealing candidate for further development. Historically, derivatives of aconitine have been found to be safe when used appropriately, and studies have suggested that these compounds are promising candidates for therapeutic use, particularly for pain management.⁸³ However, pharmacokinetic challenges related to bioavailability and CYP2D6 inhibition must be considered in further clinical development. Specifically, the CYP2D6 inhibition exhibited by these compounds, especially Sepaconitine, indicates the potential for drug-drug interactions, which could influence the metabolism of

co-administered drugs. This poses a concern for therapeutic use, as drug interactions can lead to harmful or reduced therapeutic outcomes. Therefore, careful monitoring of CYP2D6 activity during co-administration with other drugs metabolized by this enzyme is necessary to mitigate risks. Lappaconitine and Ranaconitine, like Sepaconitine, also demonstrated relatively low toxicity. However, their potential to inhibit CYP2D6 warrants a similar level of caution regarding drug-drug interactions. These findings are consistent with the safety profiles of these compounds in traditional medicine, where they have been widely used for the treatment of pain with minimal adverse effects.⁸⁴ From a pharmacokinetic perspective, these compounds face challenges in bioavailability, which is essential for their efficacy as therapeutic agents. Structural modifications could be explored to enhance bioavailability and improve their pharmacokinetic properties. For example, lipophilic modifications could help improve absorption, and the addition of functional groups could potentially reduce toxicity while enhancing target specificity.⁸⁵ Further optimization could involve prodrug strategies or the development of controlled-release formulations to ensure sustained drug action while minimizing side effects.

Pharmacophore modeling revealed detailed characteristics of the functional groups and interactions responsible for the binding of these molecules to Nav1.7, Nav1.8, and Nav1.9 sodium channels, which is important for understanding the structural motifs contributing to the high binding affinities of these ligands. The pharmacophore model showed that the amine group of sepaconitine is important for hydrophobic interactions with residues Ile1588, Phe1592, and Phe1598 in Nav1.7, and Nav1.9. These interactions stabilize the channel in a conformation that enhances binding affinity. Additionally, Sepaconitine formed hydrogen bonds with Ser1330 and Lys1333 in Nav1.8, suggesting a different binding mode that maintains a strong interaction. The benzene ring in lappaconitine is essential for hydrophobic interactions with residues in Nav1.7 and Nav1.9, such as Phe1674 and Thr1678. These interactions help to stabilize the receptor and contribute to the high binding affinity of the ligand. In Nav1.8, lappaconitine primarily acts as a hydrogen bond acceptor, indicating a different interaction paradigm that ensures strong binding.⁸⁶ Ranaconitine has a unique pharmacophore profile, with its amine group positioned to form hydrophobic contacts with Met1384 in Nav1.8 and Leu78 in Nav1.9. This is likely important for the relatively high affinity and stability of ligand binding. In Nav1.7, on the other hand, Ranaconitine predominantly forms hydrogen bonds with Tyr1671 and Thr1678, a potentially adaptive binding strategy to accommodate different sodium channel subtypes.

Pharmacokinetic and clinical translation challenges of Sepaconitine, Lappaconitine, and Ranaconitine must be carefully addressed for successful therapeutic development. While the findings from molecular docking and pharmacophore modeling demonstrate promising binding affinities for

the sodium channels Nav1.7, Nav1.8, and Nav1.9, translating these compounds into clinically viable agents requires overcoming several pharmacokinetic hurdles. Bioavailability remains a significant challenge, particularly for Lappaconitine and Ranaconitine, whose relatively high molecular weights and polar surface areas may hinder their ability to cross biological membranes effectively. In such cases, structural modifications such as increasing lipophilicity or utilizing prodrug strategies could be explored to enhance absorption and improve their pharmacokinetic profiles. Furthermore, the inhibition of CYP2D6 by Sepaconitine, Lappaconitine, and Ranaconitine presents a critical issue regarding potential drug-drug interactions. In clinical applications, careful monitoring of CYP2D6 activity will be necessary, especially when co-administering with other drugs metabolized by this enzyme, as interactions may result in altered drug efficacy or toxicity. Despite these challenges, the low toxicity profiles observed, as well as the historical use of related compounds in traditional medicine, suggest these agents could offer a relatively safe and effective solution for pain management when appropriately formulated. To ensure their clinical translation, further preclinical and clinical studies focusing on pharmacokinetics, optimal dosing strategies, and drug-drug interaction profiles will be crucial. Moreover, regulatory considerations, including adherence to guidelines for new anesthetic agents, will play an essential role in advancing these compounds from bench to bedside. Ultimately, optimization of these compounds, both in terms of their pharmacokinetic properties and their ability to minimize drug interactions, will be key for their successful development as next-generation pain therapeutics.

Limitations and future works

The primary limitation of this study is its reliance on computational methods such as molecular docking and ADME predictions. Many virtual approaches serve as useful initial insights into possible interactions and pharmacokinetic profiles but cannot fully capture the essence of experimentally conducted trials, which ultimately serve as the gold standard in drug discovery. The static models of sodium channels used in docking studies can miss out on the dynamic nature of these proteins and their interactions with other molecules in the physiological environment. Additionally, the lack of experimental data on human sodium channels necessitates further investigation to confirm the relevance of these findings to human physiology. Another issue is the risk of a possible drug-drug interaction caused by CYP2D6 inhibition of Sepaconitine, Lappaconitine, and Ranaconitine, which may hinder their clinical application. Despite the good ADME predictions, the relatively high molecular weights, including some potential Lipinski rule violations, could be a barrier to bioavailability and delivery, which requires advanced design formulations to achieve optimal therapeutic effects.

Future studies should integrate experimental validation, such as *in vitro* and *in vivo* experiments, to validate the binding affinities and therapeutic benefits of the identified compounds as well as detailed structure-activity relationship (SAR) studies to optimize these compounds for better efficacy and safety. Dynamic simulations and advanced formulation strategies should be employed to address the challenges associated with drug bioavailability and delivery. Comprehensive toxicity assessments and investigations into potential drug-drug interactions are essential for ensuring the safety and efficacy of these compounds in clinical settings. Finally, clinical trials are needed to evaluate the potential of Sepaconitine, Lappaconitine, and Ranaconitine as therapeutic agents for the treatment of painful dental pulp and to develop new anesthetic agents.

Conclusion

The present study evaluated the ability of bioactive secondary metabolites from medicinal plants to inhibit voltage-gated sodium channels (Nav1.7, Nav1.8, and Nav1.9), which cause dental pulp pain. Using various computational approaches, such as molecular docking simulations, ADME predictions, toxicity predictions, and pharmacophore modeling, three compounds, Sepaconitine, Lappaconitine, and Ranaconitine, were proposed as the best binders with excellent ADME profiles and low toxicity. Remarkably, the compounds bound in a similar manner across all sodium channel subtypes, suggesting that they could act as broad-spectrum modulators of pain signaling in dental pulp. The in-depth computational analysis helped to gain an understanding of the molecular mechanisms underlying the modulatory actions of the bioactive metabolites on sodium channels, paving the way for future experimental validation and clinical translation in dental therapy. Nevertheless, it is important to consider the fundamental limitations of computational approaches and to reinforce the fact that rigorous experimental studies are imperative to validate the therapeutic effectiveness and safety of the compounds tested in dental pulp management. Future research directions include performing further *in vitro* and *in vivo* assays, structure-activity studies, formulation optimization for dental applications, and clinical trials to evaluate the analgesic efficacy of these natural compounds in dental practice. In summary, this study demonstrated that natural products have great potential for the development of novel analgesic drugs for the treatment of painful dental pulp.

Abbreviations

ADME, absorption, distribution, metabolism, and excretion; **CASTp**, computed atlas of surface topography of proteins; **HADDOCK**, high ambiguity driven protein-protein docking; **HBA**, hydrogen bond acceptor; **HBD**, hydrogen bond donor; **LBD**, ligand-binding domains; **LGA**, Lamarckian genetic algorithm; **MlogP**, lipophilicity; **MW**, molecular weight; **SAR**, structure-activity relationship; **TPSA**, topological polar surface area. **WHO**, World Health Organization.

Acknowledgments

Acknowledgement 1: All the authors thank King Khalid University, Saudi Arabia, for the financial Support.

Acknowledgement 2: We would like to express our sincere gratitude to Doni Dermawan for his significant contributions to this research project. His expertise has been invaluable in shaping the outcome of our study..

Author contributions

Conceptualization and Methodology: Ravinder Saini, Ryan Binduhayyim.

Data Curation and Formal Analysis: Artak Heboyan.

Investigation and Resources: Ravinder Saini, Rayan Binduhayyim.

Original draft preparation: Ravinder Saini, Artak Heboyan.

Writing, Reviewing, and Editing: Mohamed Saheer.

Supervision and Project Administration: Ravinder Saini, Artak Heboyan.

Funding Acquisition: Mohamed Saheer.

Availability of data and materials

The data presented in this study are available upon request from the corresponding authors.

Declaration of conflicting interests

The author(s) declared no potential conflicts of interest with respect to the research, authorship, and/or publication of this article.

Funding

The author(s) disclosed receipt of the following financial support for the research, authorship, and/or publication of this article: The authors extend their appreciation to the Deanship of Research and Graduate Studies at King Khalid University for funding this work through Large Research Project under grant number RGP2/475/45.

Ethics approval and consent to participate

Not applicable.

Consent for publication

Not applicable.

ORCID iD

Artak Heboyan  <https://orcid.org/0000-0001-8329-3205>

Supplemental material

Supplemental material for this article is available online.

References

- González-Moles MA, González NM. Bacterial infections of pulp and periodontal origin. *Med Oral Patol Oral Cir Bucal* 2004; 9(Suppl): 34–36; 32–34.
- Renton T. Dental (odontogenic) pain. *Rev Pain* 2011; 5(1): 2–7.
- Mulpuri Y, Yamamoto T, Nishimura I, Spigelman I. Role of voltage-gated sodium channels in axonal signal propagation of trigeminal ganglion neurons after infraorbital nerve entrapment. *Neurobiol Pain* 2022; 11: 100084.
- Hameed S. Na(v)1.7 and Na(v)1.8: role in the pathophysiology of pain. *Mol Pain* 2019; 15: 1744806919858801.
- Black JA, Frézel N, Dib-Hajj SD, Waxman SG. Expression of Nav1.7 in DRG neurons extends from peripheral terminals in the skin to central preterminal branches and terminals in the dorsal horn. *Mol Pain* 2012; 8: 82.
- Shields SD, Deng L, Reese RM, Dourado M, Tao J, Foreman O, Chang JH, Hackos DH. Insensitivity to pain upon adult-onset deletion of Nav1.7 or its blockade with selective inhibitors. *J Neurosci* 2018; 38(47): 10180–10201.
- Luiz AP, Wood JN. Sodium channels in pain and cancer: new therapeutic opportunities. In: JE Barrett (ed.) *Advances in pharmacology*. Cambridge, MA: Academic Press, 2016, pp.153–178.
- Jarvis MF, Honore P, Shieh CC, Chapman M, Joshi S, Zhang XF, Kort M, Carroll W, Marron B, Atkinson R, Thomas J, Liu D, Krumbis M, Liu Y, McGaraughty S, Chu K, Roeloffs R, Zhong C, Mikusa JP, Hernandez G, Gauvin D, Wade C, Zhu C, Pai M, Scanio M, Shi L, Drizin I, Gregg R, Matulenko M, Hakeem A, Gross M, Johnson M, Marsh K, Wagoner PK, Sullivan JP, Faltynek CR, Krafte DS. A-803467, a potent and selective Nav1.8 sodium channel blocker, attenuates neuropathic and inflammatory pain in the rat. *Proc Natl Acad Sci U S A* 2007; 104(20): 8520–8525.
- Zhao C, Zhou X, Shi X. The influence of Nav1.9 channels on intestinal hyperpathia and dysmotility. *Channels (Austin)* 2023; 17(1): 2212350.
- Ma RSY, Kayani K, Whyte-Oshodi D, Whyte-Oshodi A, Nachiappan N, Gnanarajah S, Mohammed R. Voltage gated sodium channels as therapeutic targets for chronic pain. *J Pain Res* 2019; 12: 2709–2722.
- Dib-Hajj S, Black J, Waxman S. Nav1.9: a sodium channel linked to human pain. *Nat Rev Neurosci* 2015; 16(9): 511–519.
- Becker DE, Reed KL. Local anesthetics: review of pharmacological considerations. *Anesth Prog* 2012; 59(2): 90–101; quiz 102–103.
- Taylor A, McLeod G. Basic pharmacology of local anaesthetics. *BJA Edu* 2019; 20(2): 34–41.
- Roberson DP, Binshtok AM, Blas F, Bean BP, Woolf CJ. Targeting of sodium channel blockers into nociceptors to produce long-duration analgesia: a systematic study and review. *Br J Pharmacol* 2011; 164(1): 48–58.
- Sheets P, Jarecki B, Cummins T. Lidocaine reduces the transition to slow inactivation in Na(v)1.7 voltage-gated sodium channels. *Br J Pharmacol* 2011; 164: 719–730.
- Covino BG, Giddon DB. Pharmacology of local anesthetic agents. *J Dent Res* 1981; 60(8): 1454–1459.
- Su N, Wang H, Zhang S, Liao S, Yang S, Huang Y. Efficacy and safety of bupivacaine versus lidocaine in dental treatments: a meta-analysis of randomised controlled trials. *Int Dent J* 2014; 64(1): 34–45.
- Al-Dosary K, Al-Qahtani A, Alangari A. Anaphylaxis to lidocaine with tolerance to articaine in a 12 year old girl. *Saudi Pharm J* 2014; 22(3): 280–282.

19. Zhao Y, Cartabia A, Lalaymia I, Declerck S. Arbuscular mycorrhizal fungi and production of secondary metabolites in medicinal plants. *Mycorrhiza* 2022; 32(3–4): 221–256.
20. Twaij BM, Hasan MN. Bioactive secondary metabolites from plant sources: types, synthesis, and their therapeutic uses. *Int J Plant Biol* 2022; 13: 4–14.
21. Bhambhani S, Kondhare KR, Giri AP. Diversity in chemical structures and biological properties of plant alkaloids. *Molecules* 2021; 26(11): 3374.
22. Tsuchiya H. Anesthetic agents of plant origin: a review of phytochemicals with anesthetic activity. *Molecules* 2017; 22(8): 1369.
23. Siddiqui T, Sharma V, Khan MU, Gupta K. Terpenoids in essential oils: chemistry, classification, and potential impact on human health and industry. *Phytomed Plus* 2024; 4(2): 100549.
24. Masyita A, Sari RM, Astuti AD, Yasir B, Rumata NR, Emran TB, Nainu F, Simal-Gandara J. Terpenes and terpenoids as main bioactive compounds of essential oils, their roles in human health and potential application as natural food preservatives. *Food Chem X* 2022; 13: 100217.
25. Shorobi FM, Nisa FY, Saha S, Chowdhury MAH, Srisuphanunt M, Hossain KH, Rahman MA. Quercetin: a functional food-flavonoid incredibly attenuates emerging and re-emerging viral infections through immunomodulatory actions. *Molecules* 2023; 28(3): 938.
26. Semwal R, Joshi SK, Semwal RB, Semwal DK. Health benefits and limitations of rutin - a natural flavonoid with high nutraceutical value. *Phytochem Lett* 2021; 46: 119–128.
27. Dermawan D, Sumirtanurdin R, Dewantisari D. Simulasi dinamika molekular reseptor estrogen alfa dengan andrografolid sebagai anti kanker payudara. *Indones J Pharm Sci Technol* 2019; 6(2): 65–76.
28. Moradi M, Golmohammadi R, Najafi A, Moghaddam MM, Fasihi-Ramandi M, Mirnejad R. A contemporary review on the important role of in silico approaches for managing different aspects of COVID-19 crisis. *Inform Med Unlocked* 2022; 28: 100862.
29. Meng XY, Zhang HX, Mezei M, Cui M. Molecular docking: a powerful approach for structure-based drug discovery. *Curr Comput Aided Drug Des* 2011; 7(2): 146–157.
30. Dermawan D, Prabowo BA, Rakhmadina CA. In silico study of medicinal plants with cyclodextrin inclusion complex as the potential inhibitors against SARS-CoV-2 main protease (Mpro) and spike (S) receptor. *Inform Med Unlocked* 2021; 25: 100645.
31. Giordano D, Biancaniello C, Argenio MA, Facchiano A. Drug design by pharmacophore and virtual screening approach. *Pharmaceuticals (Basel)* 2022; 15(5): 646.
32. Koes D. *Pharmacophore modeling: methods and applications*. New York, NY: Springer, 2015.
33. Yamashita F, Hashida M. In silico approaches for predicting ADME properties of drugs. *Drug Metab Pharmacokinet* 2004; 19: 327–338.
34. Ursu O, Rayan A, Goldblum A, Oprea TI. Understanding drug-likeness. *Wiley Interdiscip Rev Comput Mol Sci* 2011; 1: 760–781.
35. Cavasotto CN, Scardino V. Machine learning toxicity prediction: latest advances by toxicity end point. *ACS Omega* 2022; 7(51): 47536–47546.
36. Ahuja S, Mukund S, Deng L, Khakh K, Chang E, Ho H, Shriver S, Young C, Lin S, Johnson JP Jr, Wu P, Li J, Coons M, Tam C, Brillantes B, Sampang H, Mortara K, Bowman KK, Clark KR, Estevez A, Xie Z, Verschoof H, Grimwood M, Dehnhardt C, Andrez JC, Focken T, Sutherlin DP, Safina BS, Starovasnik MA, Ortwine DF, Franke Y, Cohen CJ, Hackos DH, Koth CM, Payandeh J. Structural basis of Nav1.7 inhibition by an isoform-selective small-molecule antagonist. *Science* 2015; 350(6267): aac5464.
37. Huang X, Mukund S, Deng L, Khakh K, Chang E, Ho H, Shriver S, Young C, Lin S, Johnson JP Jr, Wu P. Structural basis for high-voltage activation and subtype-specific inhibition of human Nav1.8. *Proc Natl Acad Sci USA* 2022; 119(30): e2208211119.
38. Jumper J, Evans R, Pritzel A, Green T, Figurnov M, Ronneberger O, Tunyasuvunakool K, Bates R, Židek A, Potapenko A, Bridgland A. Highly accurate protein structure prediction with AlphaFold. *Nature* 2021; 596(7873): 583–589.
39. Guex N, Peitsch MC, Schwede T. Automated comparative protein structure modeling with SWISS-MODEL and Swiss-PdbViewer: a historical perspective. *Electrophoresis* 2009; 30(Suppl. 1): S162–S173.
40. Tian W., Chen C, Lei X, Zhao J, Liang J. CASTp 3.0: computed atlas of surface topography of proteins. *Nucleic Acids Res* 2018; 46(W1): W363–W367.
41. Saini RS, Binduhayyim RI, Gurumurthy V, Alshadidi AA, Aldosari LI, Okshah A, Kuruniyan MS, Dermawan D, Avetisyan A, Mosaddad SA, Heboyan A. Dental biomaterials redefined: molecular docking and dynamics-driven dental resin composite optimization. *BMC Oral Health* 2024; 24(1): 557.
42. Saini RS, Binduhayyim RI, Gurumurthy V, Alshadidi AA, Bavabeedu SS, Vyas R, Dermawan D, Naseef PP, Mosaddad SA, Heboyan A. In silico assessment of biocompatibility and toxicity: molecular docking and dynamics simulation of PMMA-based dental materials for interim prosthetic restorations. *J Mater Sci Mater Med* 2024; 35(1): 28.
43. van Zundert GCP, Rodrigues JP, Trellet M, Schmitz C, Kastiris PL, Karaca E, Melquiond AS, van Dijk M, De Vries SJ, Bonvin AM. The HADDOCK2.2 web server: user-friendly integrative modeling of biomolecular complexes. *J Mol Biol* 2016; 428(4): 720–725.
44. Alotaq N, Dermawan D, Elwali NE. Leveraging therapeutic proteins and peptides from lumbricus earthworms: targeting SOCS2 E3 ligase for cardiovascular therapy through molecular dynamics simulations. *Int J Mol Sci* 2024; 25(19): 10818.
45. Dermawan D, Alsenani F, Elwali NE, Alotaq N. Therapeutic potential of earthworm-derived proteins: targeting NEDD4 for cardiovascular disease intervention. *J Appl Pharm* 2024; 15(1): 216–232.
46. Xue LC, Rodrigues JP, Kastiris PL, Bonvin AM, Vangone A. PRODIGY: a web server for predicting the binding affinity of protein–protein complexes. *Bioinformatics* 2016; 32(23): 3676–3678.

47. Lazniewski M, Dermawan D, Hidayat S, Muchtaridi M, Dawson WK, Plewczynski D. Drug repurposing for identification of potential spike inhibitors for SARS-CoV-2 using molecular docking and molecular dynamics simulations. *Methods* 2022; 203: 498–510.
48. Daina A, Michielin O, Zoete V. SwissADME: a free web tool to evaluate pharmacokinetics, drug-likeness and medicinal chemistry friendliness of small molecules. *Sci Rep* 2017; 7: 42717.
49. Lai Y, Chu X, Di L, Gao W, Guo Y, Liu X, Lu C, Mao J, Shen H, Tang H, Xia CQ. Recent advances in the translation of drug metabolism and pharmacokinetics science for drug discovery and development. *Acta Pharm Sin B* 2022; 12(6): 2751–2777.
50. Alsenani F. Unraveling potential neuroprotective mechanisms of herbal medicine for Alzheimer's diseases through comprehensive molecular docking analyses. *Saudi J Biol Sci* 2024; 31(6): 103998.
51. Oxombre B, Madouri F, Journe AS, Ravez S, Woittrain E, Odou P, Duhal N, Ninni S, Montaigne D, Delhem N, Vermersch P. Safe and efficient sigma1 ligand: a potential drug candidate for multiple sclerosis. *Int J Mol Sci* 2022; 23(19): 11893.
52. Sander T, Freyss J, Von Korff M, Rufener C. DataWarrior: an open-source program for chemistry aware data visualization and analysis. *J Chem Inf Model* 2015; 55(2): 460–473.
53. Lipinski CA. Lead- and drug-like compounds: the rule-of-five revolution. *Drug Discov Today Technol* 2004; 1: 337–341.
54. Shahab M, de Farias Morais GC, Akash S, Fulco UL, Oliveira JI, Zheng G, Akter S. A robust computational quest: discovering potential hits to improve the treatment of pyrazinamide-resistant *Mycobacterium tuberculosis*. *J Cell Mol Med* 2024; 28(8): e18279.
55. Shah M, Khan F, Ahmad I, Deng CL, Perveen A, Iqbal A, Nishan U, Zaman A, Ullah R, Ali EA, Chen K. Computer-aided identification of *Mycobacterium tuberculosis* resuscitation-promoting factor B (RpfB) inhibitors from *Gymnema sylvestre* natural products. *Front Pharmacol* 2023; 14: 1325227.
56. Kaserer T, Beck KR, Akram M, Odermatt A, Schuster D. Pharmacophore models and pharmacophore-based virtual screening: concepts and applications exemplified on hydroxysteroid dehydrogenases. *Molecules* 2015; 20(12): 22799–22832.
57. Muchtaridi M, Dermawan D, Yusuf M. Molecular docking, 3D structure-based pharmacophore modeling, and ADME prediction of alpha mangostin and its derivatives against estrogen receptor alpha. *J Young Pharm* 2018; 10(3): 252–259.
58. Wolber G, Langer T. LigandScout: 3-D pharmacophores derived from protein-bound ligands and their use as virtual screening filters. *J Chem Inf Model* 2005; 45(1): 160–169.
59. Langer T, Hoffmann R. Pharmacophore modelling: applications in drug discovery. *Expert Opin Drug Discov* 2006; 1: 261–267.
60. Galeotti N, Mannelli LDC, Mazzanti G, Bartolini A, Ghelardini C. Menthol: a natural analgesic compound. *Neurosci Lett* 2002; 322(3): 145–148.
61. Gaudio C, Hao J, Martin-Eauclaire MF, Gabriac M, Delmas P. Menthol pain relief through cumulative inactivation of voltage-gated sodium channels. *Pain* 2012; 153(2): 473–484.
62. Ghelardini C, Galeotti N, Salvatore G, Mazzanti G. Local anaesthetic activity of the essential oil of *Lavandula angustifolia*. *Planta Med* 1999; 65(8): 700–703.
63. Leal-Cardoso JH, da Silva-Alves KS, Ferreira-da-Silva FW, dos Santos-Nascimento T, Joca HC, de Macedo FH, de Albuquerque-Neto PM, Magalhães PJ, Lahlou S, Cruz JS, Barbosa R. Linalool blocks excitability in peripheral nerves and voltage-dependent Na⁺ current in dissociated dorsal root ganglia neurons. *Eur J Pharmacol* 2010; 645(1–3): 86–93.
64. Ghelardini C, Galeotti N, Mazzanti G. Local anaesthetic activity of monoterpenes and phenylpropanes of essential oils. *Planta Med* 2001; 67(6): 564–566.
65. Dolara P, Corte B, Ghelardini C, Pugliese AM, Cerbai E, Menichetti S, Nostro AL. Local anaesthetic, antibacterial and antifungal properties of sesquiterpenes from myrrh. *Planta Med* 2000; 66(4): 356–358.
66. Ghelardini C, Galeotti N, Mannelli LDC, Mazzanti G, Bartolini A. Local anaesthetic activity of beta-caryophyllene. *Farmacol* 2001; 56(5–7): 387–389.
67. Turabekova MA, Rasulev BF, Dzhakhangirov FN, Toropov AA, Leszczynska D, Leszczynski J. Aconitum and delphinium diterpenoid alkaloids of local anesthetic activity: comparative QSAR analysis based on GA-MLRA/PLS and optimal descriptors approach. *J Environ Sci Health C Environ Carcinog Ecotoxicol Rev* 2014; 32(3): 213–238.
68. Gutser UT, Fries J, Heubach JF, Matthiesen T, Selve N, Wilffert B, Gleitz J. Mode of antinociceptive and toxic action of alkaloids of *Aconitum spec.* *Naunyn Schmiedeberg's Arch Pharmacol* 1998; 357(1): 39–48.
69. Wang CF, Gerner P, Wang SY, Wang GK. Bulleyaconitine A isolated from aconitum plant displays long-acting local anesthetic properties in vitro and in vivo. *Anesthesiology* 2007; 107(1): 82–90.
70. Nakashima RA, Garlid KD. Quinine inhibition of Na⁺ and K⁺ transport provides evidence for two cation/H⁺ exchangers in rat liver mitochondria. *J Biol Chem* 1982; 257(16): 9252–9254.
71. Wu YL, Ohsaga A, Oshiro T, Iinuma K, Kondo Y, Ebihara S, Sasaki H, Maruyama Y. Suppressing effects of red wine polyphenols on voltage-gated ion channels in dorsal root ganglionic neuronal cells. *Tohoku J Exp Med* 2005; 206(2): 141–150.
72. Kim TH, Lim JM, Kim SS, Kim J, Park M, Song JH. Effects of (-) epigallocatechin-3-gallate on Na⁺ currents in rat dorsal root ganglion neurons. *Eur J Pharmacol* 2009; 604(1–3): 20–26.
73. Adaramoye OA. Protective effect of kolaviron, a biflavonoid from *Garcinia kola* seeds, in brain of Wistar albino rats exposed to gamma-radiation. *Biol Pharm Bull* 2010; 33(2): 260–266.
74. Kim HI, Kim TH, Song JH. Resveratrol inhibits Na⁺ currents in rat dorsal root ganglion neurons. *Brain Res* 2005; 1045(1–2): 134–141.
75. Gao X, Hu J, Zhang X, Zuo Y, Wang Y, Zhu S. Research progress of aconitine toxicity and forensic analysis of aconitine poisoning. *Forensic Sci Res* 2020; 5(1): 25–31.
76. Li TF, Fan H, Wang YX. Aconitum-derived bulleyaconitine A exhibits antihypersensitivity through direct stimulating dynorphin A expression in spinal microglia. *J Pain* 2016; 17(5): 530–548.

77. Turabekova MA, Rasulev BF, Levkovich MG, Abdullaev ND, Leszczynski J. Aconitum and Delphinium sp. alkaloids as antagonist modulators of voltage-gated Na⁺ channels. AM1/DFT electronic structure investigations and QSAR studies. *Comput Biol Chem* 2008; 32(2): 88–101.
78. Salehi A, Ghanadian M, Zolfaghari B, Jassbi AR, Fattahian M, Reisi P, Csopor D, Khan IA, Ali Z. Neuropharmacological potential of diterpenoid alkaloids. *Pharmaceuticals (Basel)* 2023; 16(5): 747.
79. Kerns E, Di L. *Drug-like properties: concept, structure design and methods, from ADME to toxicity optimization*. Cambridge, MA: Academic Press, 2008.
80. Guengerich FP. Cytochrome p450 and chemical toxicology. *Chem Res Toxicol* 2008; 21(1): 70–83.
81. Leeson PD, Springthorpe B. The influence of drug-like concepts on decision-making in medicinal chemistry. *Nat Rev Drug Discov* 2007; 6(11): 881–890.
82. Waring MJ. Lipophilicity in drug discovery. *Expert Opin Drug Discov* 2010; 5(3): 235–248.
83. Chan YT, Wang N, Feng Y. The toxicology and detoxification of Aconitum: traditional and modern views. *Chin Med* 2021; 16(1): 61.
84. Knisely MR, Carpenter JS, Draucker CB, Skaar T, Broome ME, Holmes AM, Von Ah D. CYP2D6 drug-gene and drug-drug-gene interactions among patients prescribed pharmacogenetically actionable opioids. *Appl Nurs Res* 2017; 38: 107–110.
85. Kadela-Tomanek M, Jastrzębska M, Marciniak K, Chrobak E, Bębenek E, Boryczka S. Lipophilicity, pharmacokinetic properties, and molecular docking study on SARS-CoV-2 target for betulin triazole derivatives with attached 1,4-quinone. *Pharmaceutics* 2021; 13(6): 781.
86. Lipkind GM, Fozzard HA. Molecular modeling of local anesthetic drug binding by voltage-gated sodium channels. *Mol Pharmacol* 2005; 68(6): 1611–1622.